ATLAS Internal Note
ATL-MUON-2001-xxx
ALICE Internal Note
ALICE-INT-2001-xxx
September 2001

The ALMY Sensor Modules

F. Bauer [a1], V .Danielyan [a,b], S .Horvat [a2], H.Kroha [a]

a) Max-Planck-Institut für Physik, Munich, Germany
b) Yerevan Physics Institute, Yerevan, Armenia

---

[1] Also at CEA Saclay, DSM, DAPNIA, Gif-sur-Yvette, France

[2] On leave of absence from Ruđer Bošković Institute, Zagreb, Croatia

INTRODUCTION

The desired performance of modern large area tracking detectors can only be achieved by precise monitoring of the relative positions of the detector components. For example in the muon spectrometer of the ATLAS experiment at the LHC, an optical alignment system has to provide the misalignment corrections to the track curvature with an accuracy of 30 μm (RMS).

A novel optical laser alignment monitoring system ("ALMY System"), developed for such applications, monitors the alignment of several semi-transparent optical position sensors along a collimated laser beam. The principle is shown in Fig.1.

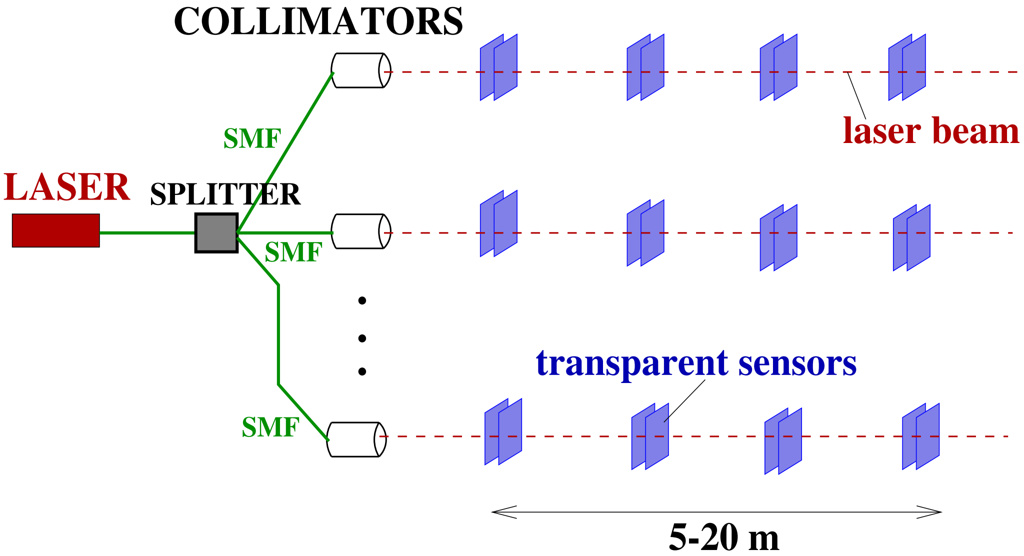

Fig.1. Principle of the ALMY laser alignment monitoring system with semi-transparent position sensors and a light distribution system with single-mode optical fibers (SMF).

The GaAlAs laser diodes emit the visible light at 690 nm and 780 nm wavelength. The beams are collimated via single-mode optical fibers and have a Gaussian beam profile with 2-5 mm diameter over a 15 m distance. The laboratory tests and the tests at the TESLA Free Electron Laser facility demonstrate that more than 10 sensors can be aligned along a 780 nm laser beam.

The layout of an ALMY sensor is shown in Fig.2. The sensor consists of a 0.3-1 μm thick layer of hydrogenated amorphous silicon (a-Si:H) between the two orthogonally segmented indium-tin-oxide (ITO) electrode layers which cover the sensitive area of 20x20 mm^2. The top 64 strip electrodes act as Schottky contacts, with 64 ground electrodes at the bottom. Such a layout allows for a two-dimensional position measurement. The active sensor layer is deposited on the 0.5-1 mm thick glass substrate, with an additional anti-reflective coating on the back side of the glass (10 cm diameter glass wafers are cut into 7 sensor substrates). A transmittance of 90%(75%) has been achieved with the 780 nm (690 nm) lasers. In the last several years extensive tests have been performed on 150 ALMY I and ALMY II sensor modules with integrated readout electronics (see Fig.3.). The results are described in the first section of this note. The system with ALMY II modules has been tested for the performance in the ATLAS end-cap muon spectrometer (section II). Section III describes the performance of the new, recently developed, readout electronics (ALMY III modules).

The recent changes also include the improvements in the production of the glass substrates.

Deposition of the active a-Si:H cell onto the new substrates is under development, the thicknesses of various layers still to be optimized. The most recent results and the performance of the new sensor cells with ALMY III electronics is outlined in the section IV. Section V describes the influence of the long-term laser illumination of a sensor on the changes in its sensitivity and the position resolution. The results of the radiation hardness tests are outlined in the section VI.

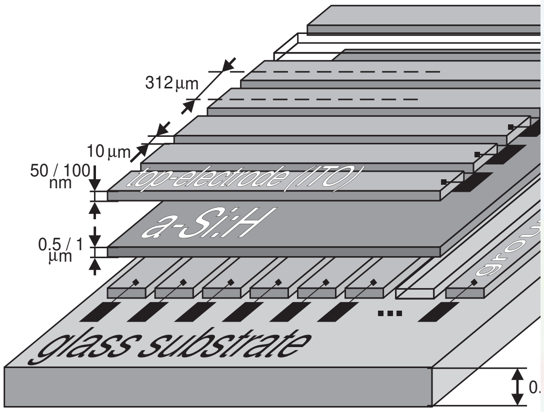

Fig.2. Layout of an amorphous silicon strip sensor.

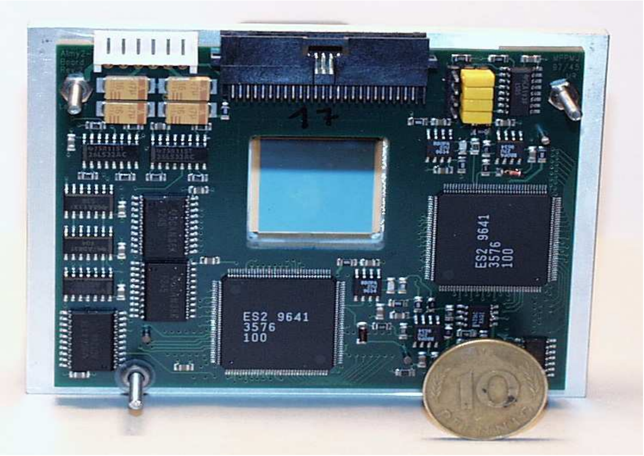

Fig.3. ALMY sensor module with integrated readout electronics.

I. ALMY II SENSOR PERFORMANCE

Fig.4. shows the typical current-voltage characteristics of the ALMY II sensor diodes, characterized by a low dark current of 10^{-9} to 10^{-7}A/cm^2.

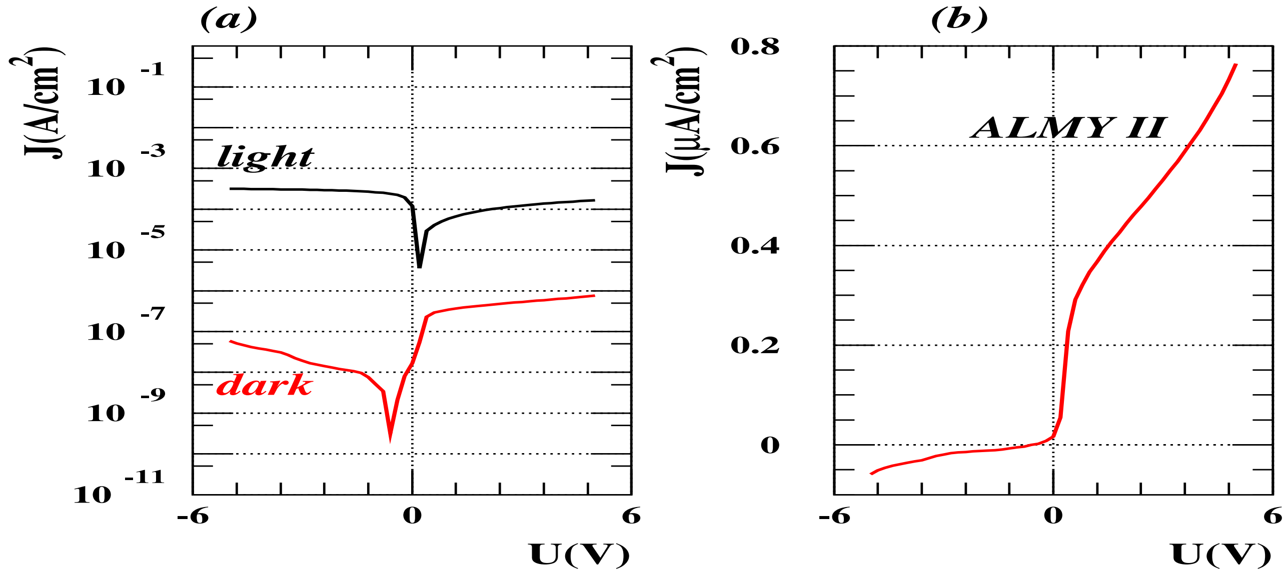

Fig.4. Current-voltage characteristics of the ALMY II Schottky diodes. (a) Measurements on the illuminated cell (light) and non-illuminated cell (dark) are shown in a logarithmic scale. (b) Measurement on a non-illuminated cell is also presented in a linear scale.

The anti-reflective coating on the back side of the glass substrate reduces the reflectivity of the glass surface to less than 0.5%, thus making the interference effects negligible. In this way the variations in the sensors position measurement are avoided. A uniform position resolution of 1 μm has been achieved over the whole active surface (see Fig.5.)

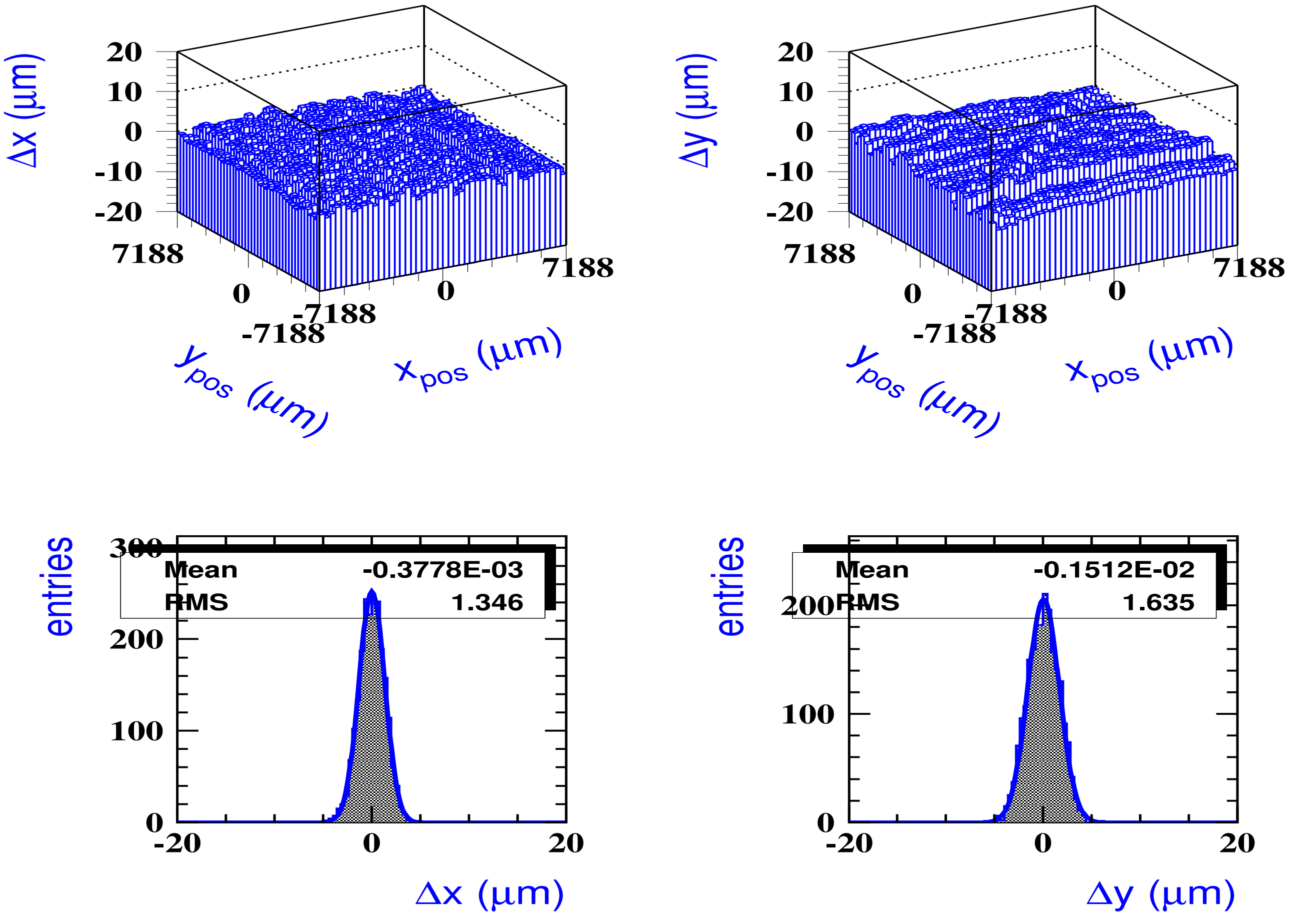

Fig.5. Position resolution (Δx, Δy) of an a-Si:H sensor with anti-reflective coating in the two coordinates (x_{pos}, y_{pos}).

The position resolution is insensitive to high magnetic fields due to the low Hall conductivity of amorphous silicon ($\mu_n^H = 10^{-2} - 10^{-3}$ cm^2/Vs).

The finite wedge angle and the curvature of the glass substrate can introduce the uncertainties in the refraction of the traversing laser beam. However, the beam refraction angle can be measured in a scan of the sensor surface and used as a senor parameter. The uncertainties are then reduced to less than 3 μrad (see Fig.6.).

II. PERFORMANCE IN ATLAS END-CAP MUON SPECTROMETER

Fig.7. shows the polar alignment rays connecting the MDT chambers in three to four different stations of the ATLAS end-cap muon spectrometer.

The rays have to provide the misalignment corrections of $\sim$30 μm to muon track sagitta, as well as to measure the angular displacements with the precision of ~ 50 μrad. The performance of an ALMY system along one of such alignment rays (the polar monitor) has been extensively tested.

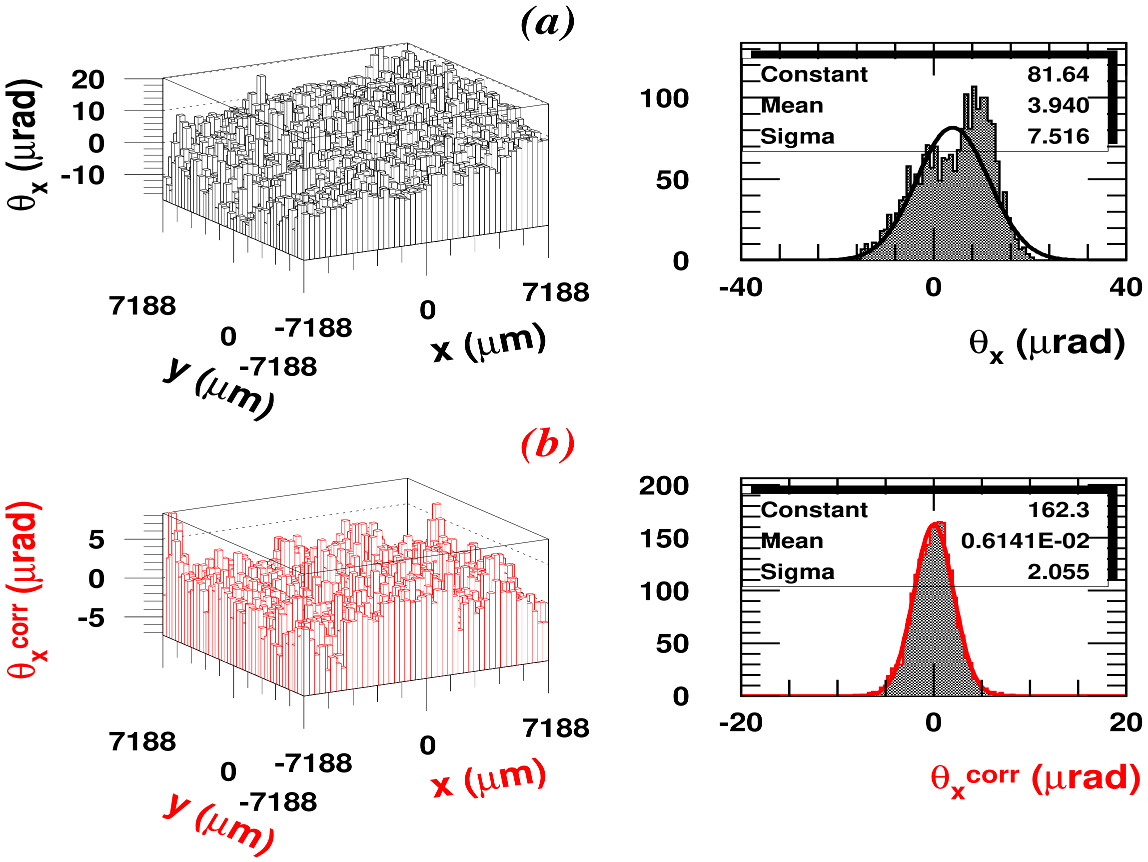

Fig.6. Laser beam refraction angle for a sensor with the glass substrate of a finite wedge angle (a) ϑ_x before and (b) $\vartheta_x{}^{corr}$ after the calibration parameters are applied. Similar result is also obtained for the y-component.

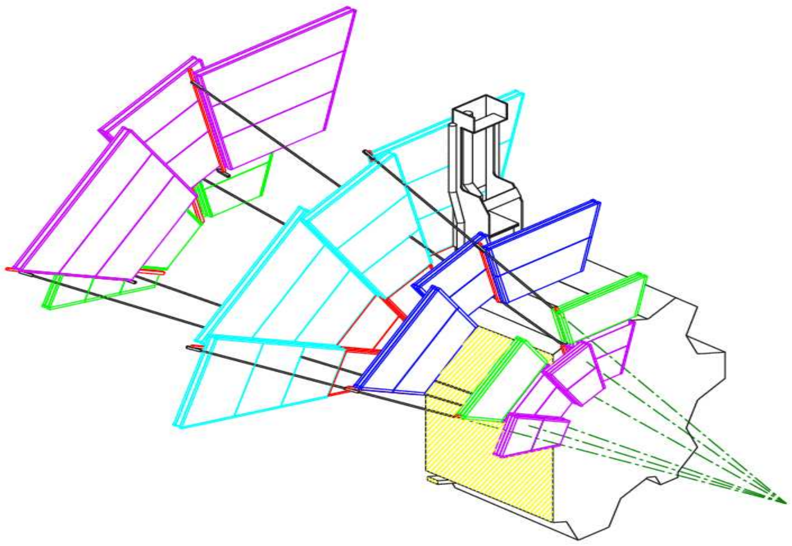

Fig.7. Polar alignment rays in one octant of the ATLAS end-cap muon spectrometer, connecting the MDT chambers of all three (four) muon stations.

The polar monitor consists of three ALMY telescopes along one laser beam, one for each of the muon stations. ALMY telescope (see Fig.8.) is assembled of two ALMY modules mounted parallel to each other at distance of 10 cm. It measures the laser beam position and the angular direction of the beam.

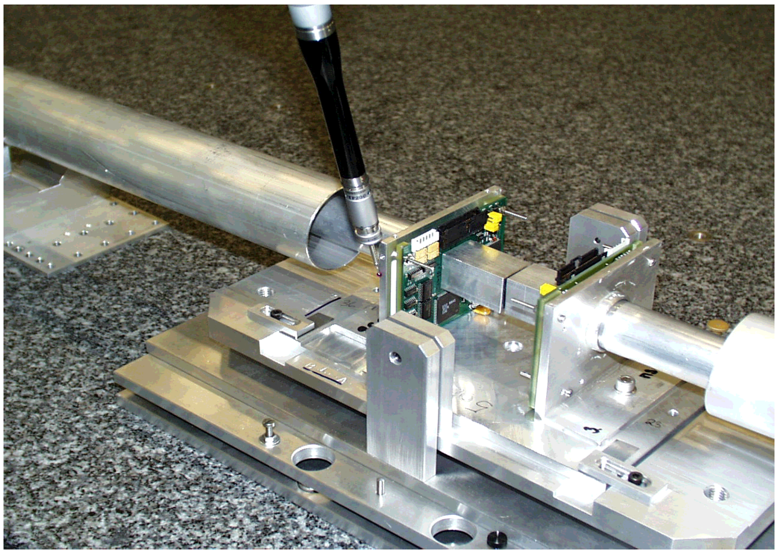

Fig.8. ALMY telescope for the measurement of the laser beam position and direction. It consists of two ALMY sensors mounted parallel to each other at the distance of 10 cm.

Fig.9 shows the setup for the performance tests.

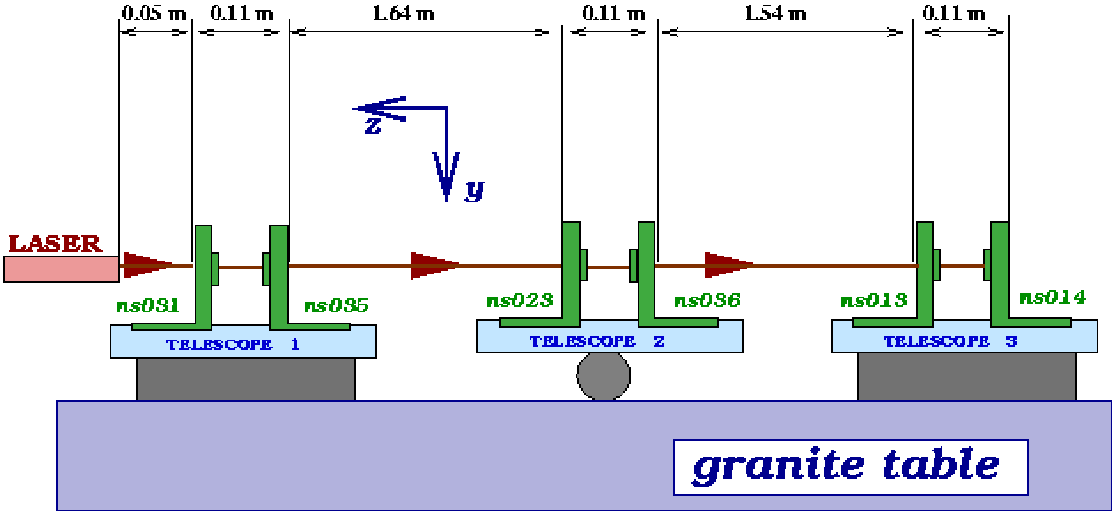

Fig.9. Setup for the absolute performance test of an ALMY polar monitoring system for ATLAS end-cap muon spectrometer.

Two independent measurements are made: the local laser beam position is measured by the ALMY sensors, and the global sensor coordinates are determined using the 3D Coordinate Measuring Machine. The comparison of these two measurements gives the information about the absolute sensor performance. The middle telescope can be tilted around the x- and y-axis, allowing to test the angular resolution of the telescope. Eight different angular orientations are tested, each using nine different laser beam directions. Fig.10. shows the outcome for the sagitta resolution and an angular resolution of a described setup.

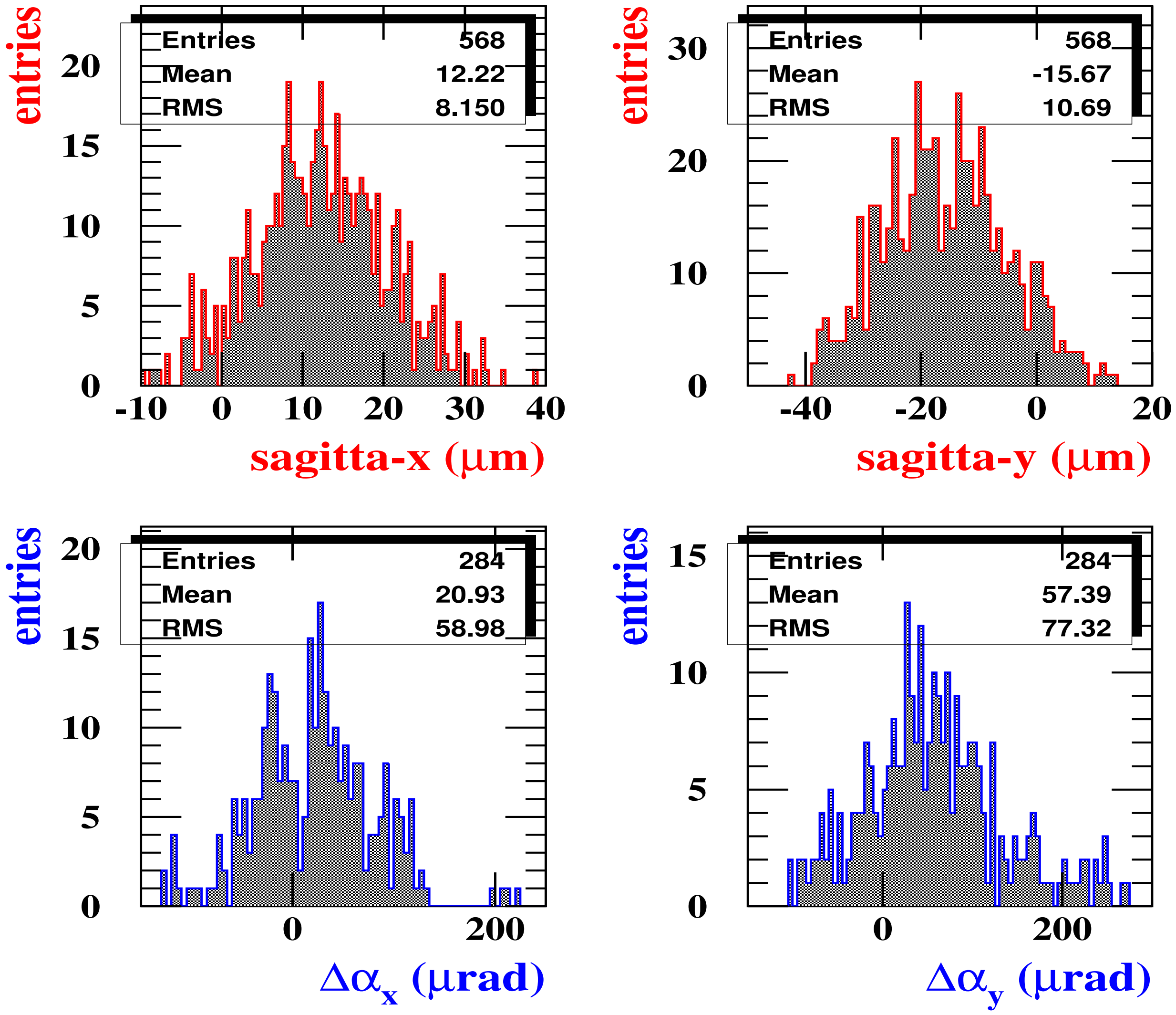

Fig.10. Sagitta resolution (μm) and the angular resolution $\Delta\alpha_x$, $\Delta\alpha_y$ (μrad) of an ALMY polar monitor in the ATLAS end-cap muon spectrometer.

The false sagitta resolution is ~20 μm, which is well within the specified requirements. The angular resolution of 60-80 μrad still has to be improved (50 μrad r.m.s. required) by using a twice larger telescope lever arm. The test has also demonstrated the efficiency of the calibration procedure (i.e. corrections due to the the laser beam refraction).

Additional test performed with a 14m long laser beam demonstrated the stability and the straightness of the beam, independent of the air turbulence around it.

III. ALMY III ELECTRONIC BOARDS

The new ALMY III sensor electronics (see Fig.11.) is currently in the last stages of development. It has an advantage of smaller outline dimensions (60x60 mm^2). The new design is more reliable - no trimming potentiometers are needed, there is no need for a regulated power supply and the power dissipation is decreased by a factor of 6. The more detailed description can be found in the Appendix to this note.

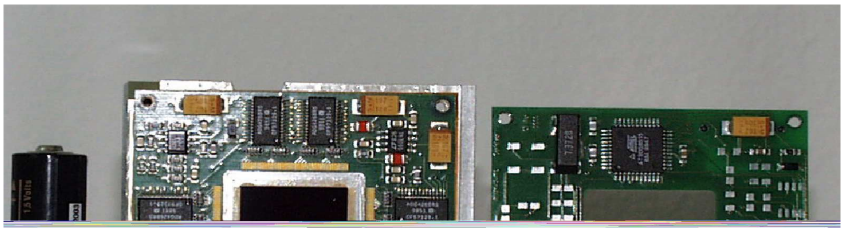

Fig.11. New ALMY electronic boards (analog board on the lefthand and the digital one on the righthand side).

Fig.12. shows the position resolution distribution obtained using the ALMY III readout electronics. No cross-talk effects are observed and the distribution is uniform over the whole sensor surface.

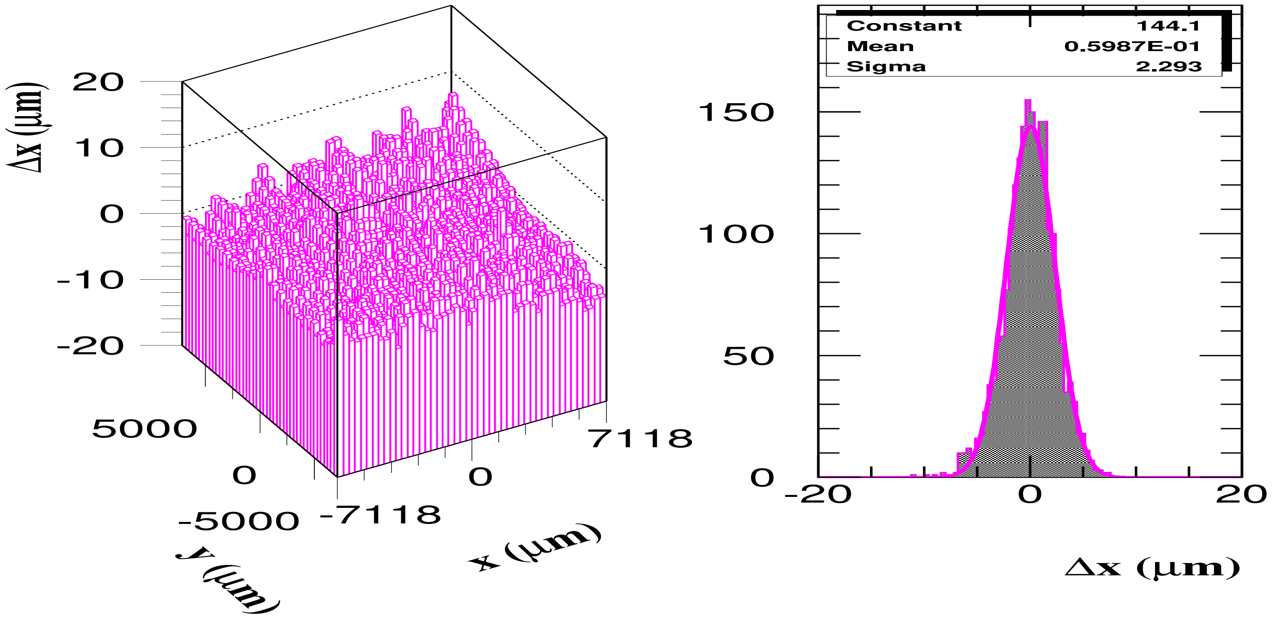

Fig.12. Position resolution Δx (μm) of an old a-Si-H sensor with the new ALMY III readout electronics. Similar distribution is obtained for y-direction as well.

IV. ALMY III MODULES WITH NEW SENSOR CELLS

As from recently the calibration procedure (needed for reducing the uncertainties in the laser beam refraction) can be avoided by using the high-quality polished parallel glass wafers for sensor fabrication. Fig.13. shows the refraction angle distribution for a typical 10 cm diameter glass wafer. The average beam refraction and the beam refraction error are both below the 3 μrad.

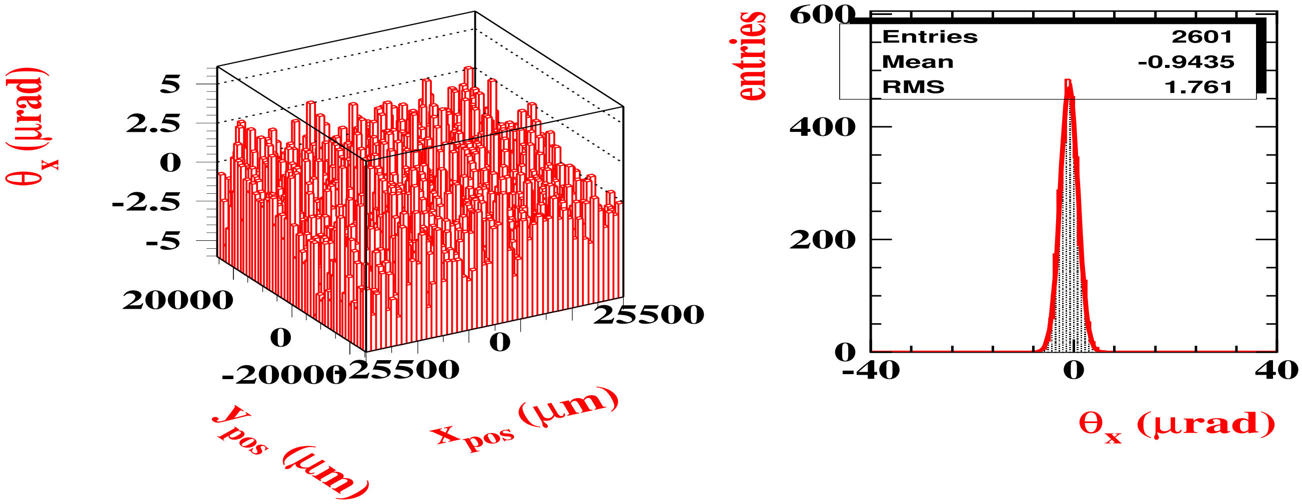

Fig.13. Laser beam refraction angle distribution from a scan of a 10 cm diameter glass wafer (for simplicity only the x-component, ϑ_x, is shown).

The deposition of the active sensor surface on the new high quality polished glass wafers is still in a (late) development stage, the thicknesses of the various layers still to be optimized. Fig.14. shows the typical current-voltage characteristics of these sensor cells.

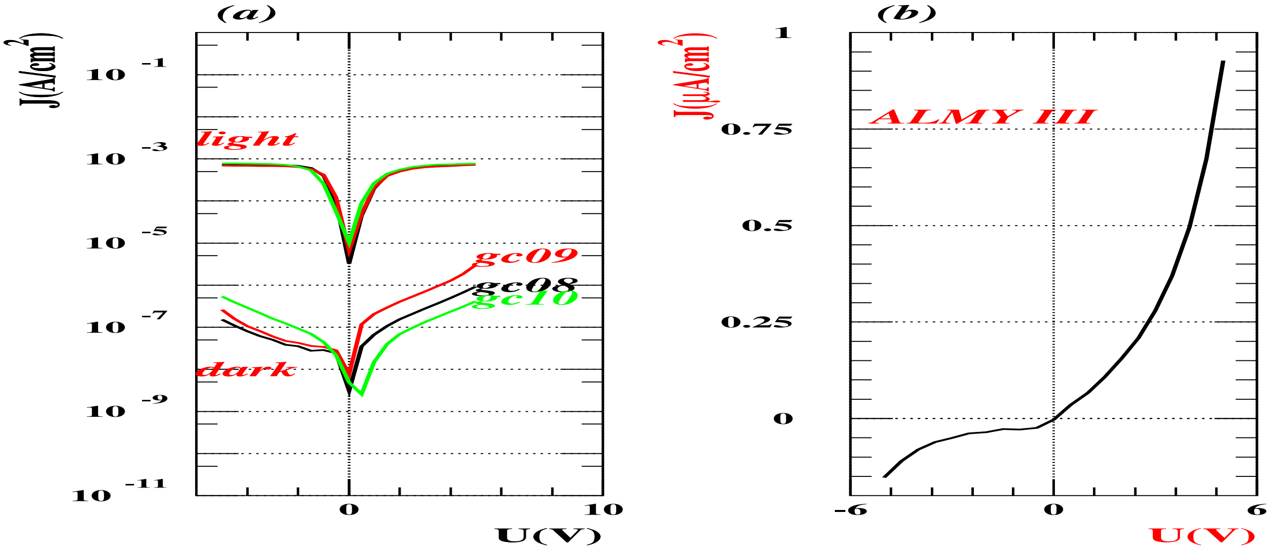

Fig.14. Current-voltage characteristics measured on the diodes of the new a-Si:H sensor cells (for three glass wafers - gc08, gc09 and gc10). (a) Measurement on the illuminated cell (light) and non-illuminated cell (dark) are shown in a logarithmic scale. (b) Measurement on a non-illuminated cell is also presented in a linear scale.

The dark current measured at the bias voltage of 1V is uniformly distributed over all sensor strips (see Fig.15.)

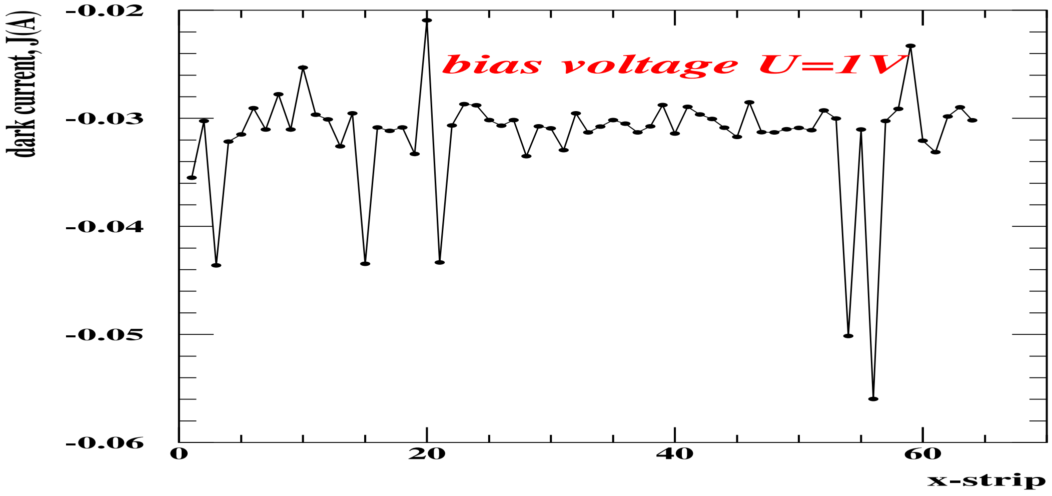

Fig.15. Dark current distribution over the sensor strips, at bias voltage of 1V, for the newly produced sensor cells

The performance of the ALMY III sensor modules with the newly produced sensor cells is shown on Fig.16. and Fig.17. The position resolution of $\sim 3\,\mu m$, the refraction angle of less than 3 μrad (without calibration procedure), the transmittance of 84% and a uniform sensor sensitivity to illumination are observed.

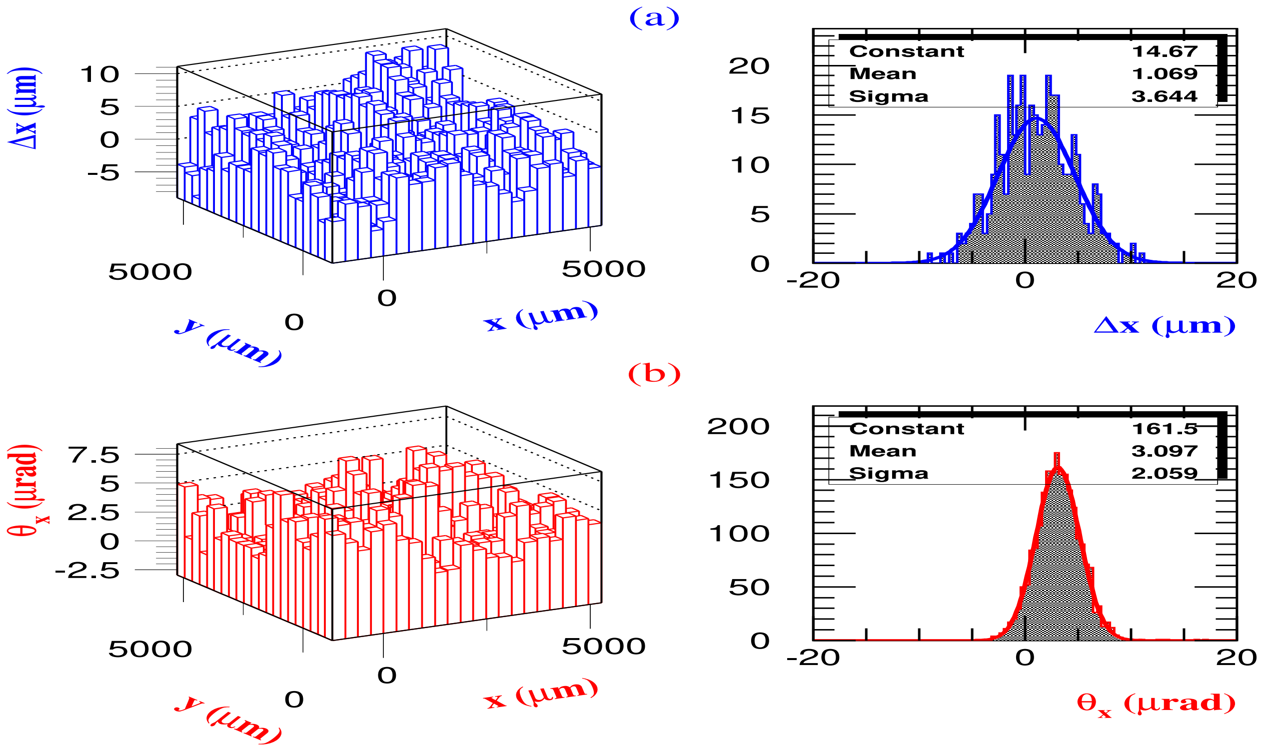

Fig.16. (a) Position resolution Δx and (b) refraction angle ϑ_x (no calibration corrections applied) of an ALMY III module with newly produced sensor cell on a polished parallel glass substrate.

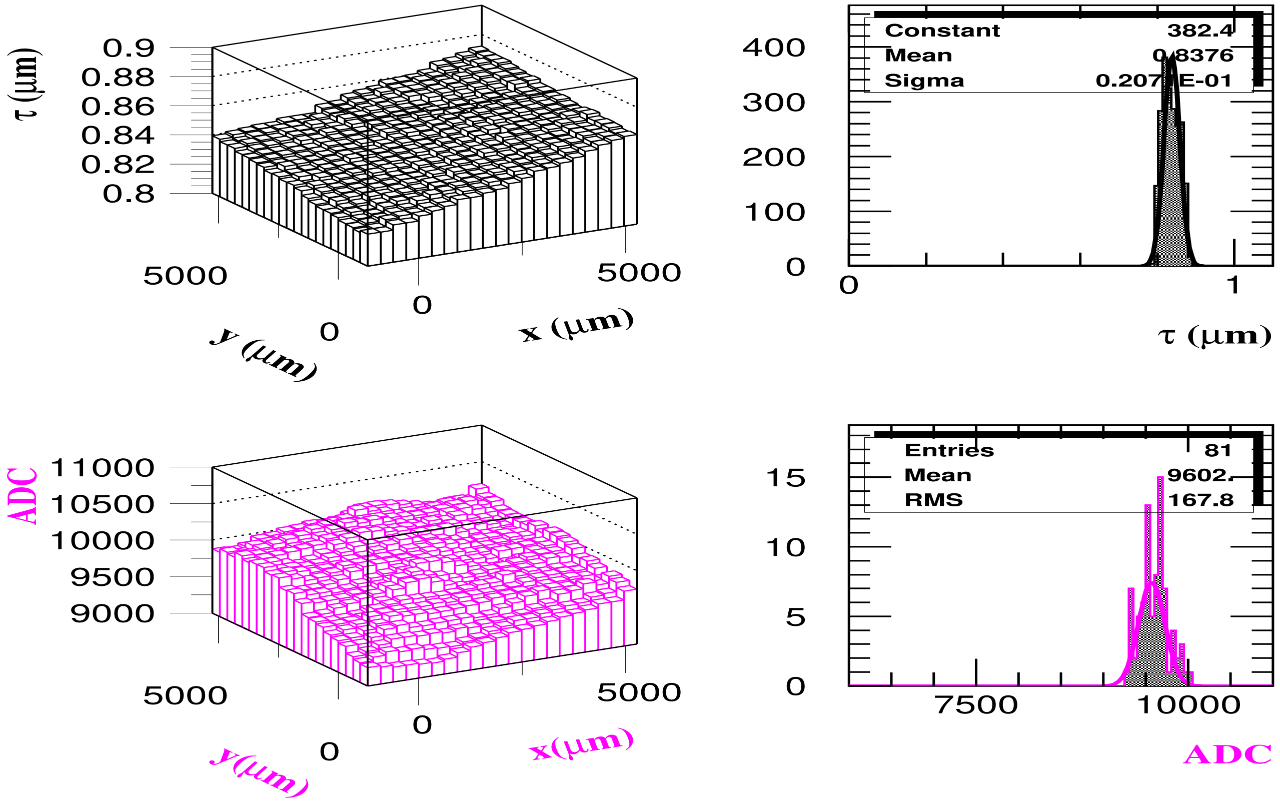

Fig.17. (a)Transmission (τ) and (b) sensitivity (ADC) of an ALMY III module with newly produced sensor cell on a polished parallel glass substrate.

V. AGING STUDIES

It is observed in the studies of the solar cells that the sensitivity of a-Si:H deteriorates under illumination. Thus, the effect of the long-term illumination on the performance of ALMY sensors needed to be investigated. After several hours of illumination of an ALMY II module with a 690 nm laser beam of 3 mm diameter and 10 mW/cm^2 intensity the local sensitivity degradation causes significant errors in the position measurement (see Fig.18.). The effect is also referred to as the aging effect.

However, in the normal operation mode, using a 780 nm laser beam of 10 mW/cm^2 intensity (giving the maximum unsaturated signal) the degradation is reduced to a tolerable rate. After 500 hours of continuous illumination the sensitivity loss measured on 4 different sensors is only 2% (see Fig.19.). This corresponds to the local position measurement error of ¡5 μm after 20 years of operation in the ATLAS muon spectrometer.

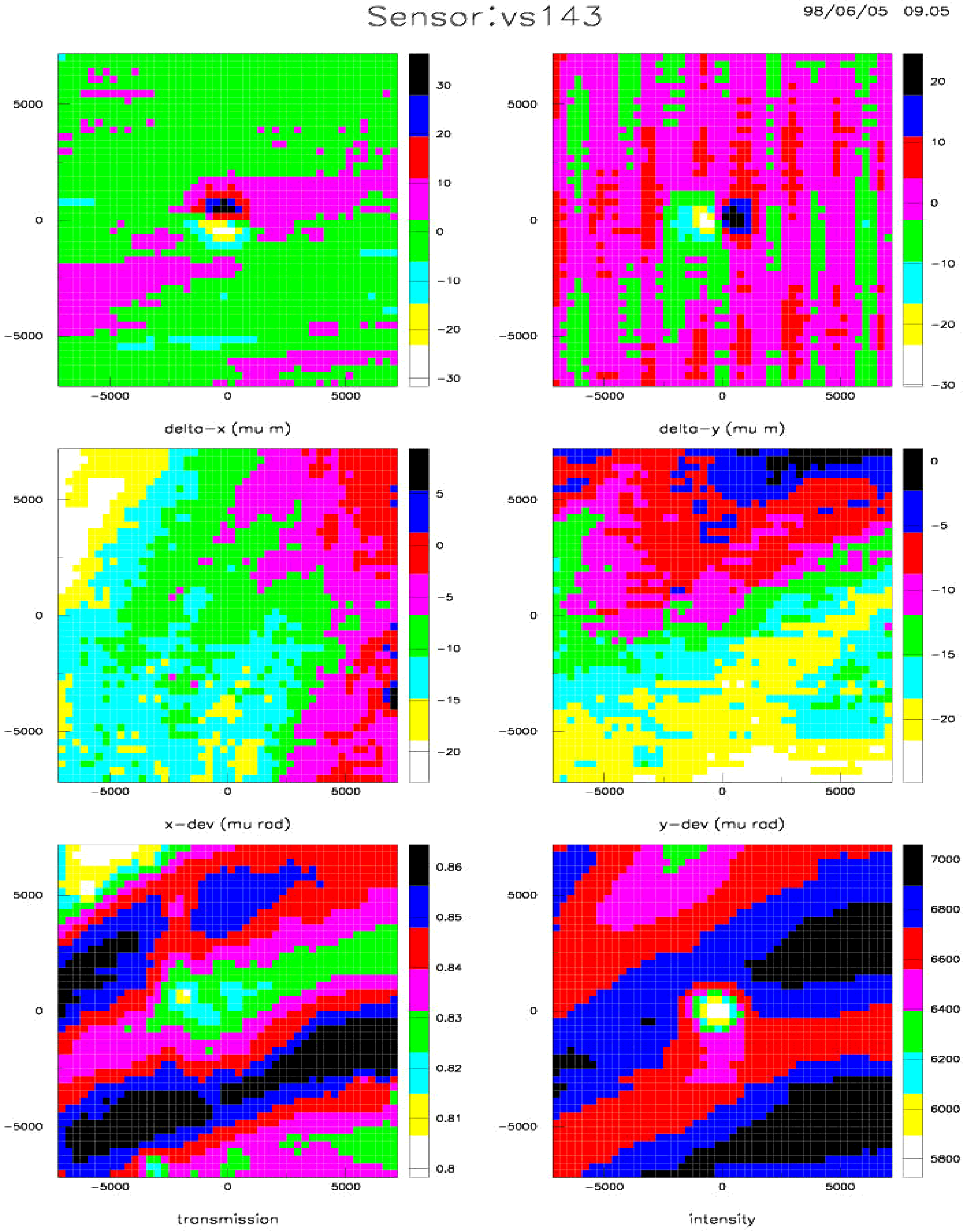

Fig.18. The scan of the sensor surface shows the local degradation of the sensitivity (relative light intensity) and of the position resolution Δx, Δy (μm) after several hours of illumination with a 690 nm laser beam (10 mW/cm^2 intensity). The transmittance and the beam refraction angle (μrad) are not affected by illumination.

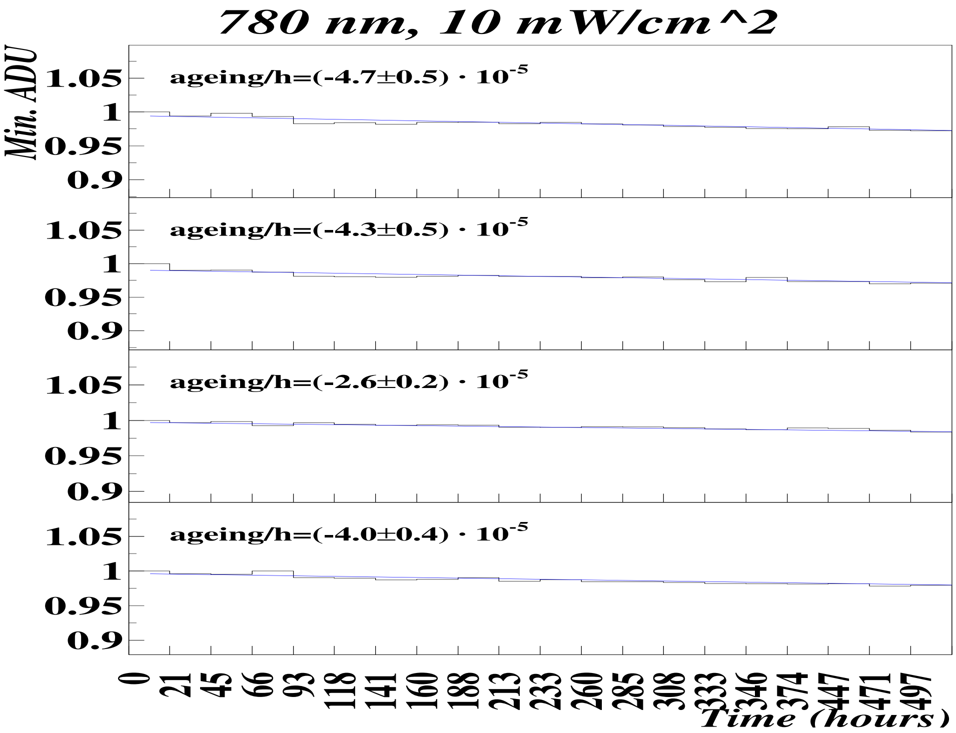

Fig.19. Long-term monitoring of the sensitivity loss on 4 ALMY sensors under illumination with 780 nm laser beam of 3 mm diameter and 10 mW/cm^2 intensity.

At the wavelength of 690 nm the sensitivity of a-Si:H is 10 times higher than at 780 nm, implying that the aging effect observed with 780 nm laser shouldn't increase when the ALMY system is operated using 690 nm laser beams of ten times lower intensity. This is demonstrated by illuminating one sensor continuously for 1500 hours with a 690 nm laser beam of 1 mW/cm^2 intensity. The sensitivity degradation of only 2% was observed (see Fig.20.) indicating the possibility to operate the system using the visible light.

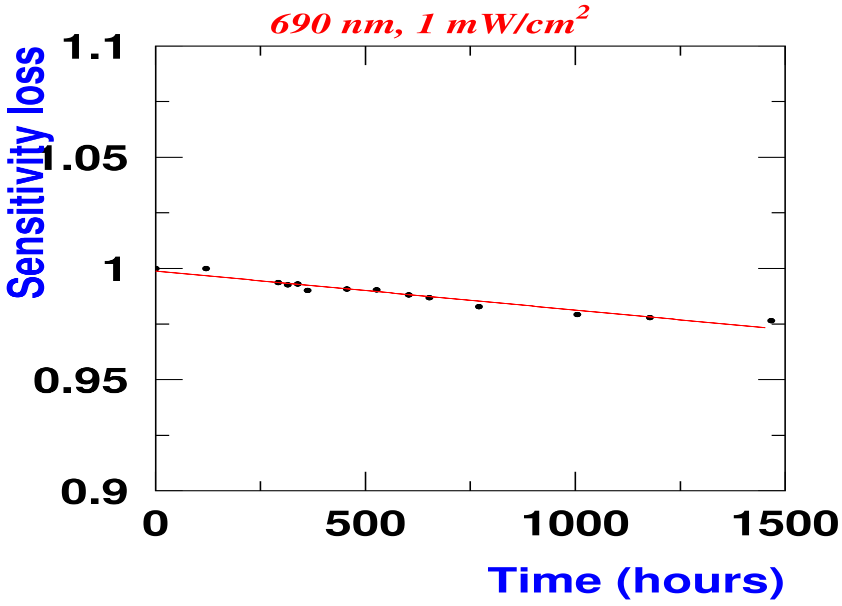

Fig.20. Long-term monitoring of the sensitivity degradation of a-Si:H sensor under illumination with a 690 nm

laser beam of 3 mm diameter and 1 mW/cm^2 intensity.

ACKNOWLEDGMENTS

The development of the sensor readout electronics was partially supported by INTAS-CERN project 99-0118.

REFERENCES

APPENDIX

ALMY III SENSOR ELECTRONICS

New ALMY sensor (ALMY-VN) electronics consists of two printed circuit boards (PCB) ALMY-VN and ALMY-V-IFC . ALMY-VN (see almy-vn scheme) board contains all analog circuits. Below they are listed with brief description.

* Resistor networks R1...R16. Through this resistors are closed photocurrent paths.

* Analog multiplexers U1...U8. U1, U2 are used for multiplexing signals from X strips with odd numbers (X01, X03, X63) and U3, U4 for even numbered X strips (X02, X04, X64). Similarly U5, U6 are used for odd numbered Y strips and U7, U8 - for even numbered Y strips. One can see, that corresponding of the strip numbers and multiplexer inputs is not straight. For example, X01 is connected to U1:S8 input, X03 to U1:S7 and so on descending until X15 to U1:S1, but then X17 is connected to U1:S9, X19 to U1:S10 and so on, ascending until X31 to U1:S16. Such inhomogeneous connection is chosen to optimize the PCB layout. Multiplexer addresses are switched by microcontroller and it can be done in arbitrary sequence.
* Voltage divider for X strips biasing: R17, R18, C1, and C2. Currently the bias voltage is set equal to approximately 1 Volt, but the setting can be easily changed, by using another value for R18 resistor. The buffer capacitor C2 should be large enough to prevent the bias voltage deviation, caused by current through R21 resistor, which is changing according to the selected strip photocurrent (the voltage on U9:6 pin is always equal to the one on the U9:5, which is proportional to X strip photocurrent). In previous versions of ALMY sensor this deviation brought to crosstalk between X and Y coordinates.

* X transimpedance amplifier on U9 and Y transimpedance amplifier on U10. The second stage of the X amplifier shifts signal level from the bias voltage to ground. Therefore R21 should be equal to R20, and R22 to R23. As the amplifiers are of transimpedance type, their gain is measured in impedance (resistance) units. The gains of X and Y amplifiers are equal and can be calculated by formulas:
Xgain = R19*(R22/R21) = 3900000 Ohm = 3.9V/μA
Ygain = R26*(R28/R27) = 3.9V/μA

* Analog to Digital Converter (ADC) U11. This is 12-bit 4-channel ADC with internal reference voltage of 2V, which corresponds to maximal code value of 4095. Except of the main measured voltages of X and Y coordinates, there is possibility for diagnostic purposes to measure values of Vbias and Vss (the negative supply voltage). Having 4 times larger dynamic range, we can choose large enough zero shifting of amplifiers outputs, to prevent negative values for the worst conditions: an operational amplifiers with maximal input voltage offset values, working at maximal or minimal rated temperatures. These zero shifts are made by R24, R25 divider for X and R29, R30 for Y and are equal about 190-200 channels (of 4095) for amplifiers with zero input voltage offset. D1 and D2 Schottky diodes protect the ADC inputs from negative polarity transients.

* Inductorless low-noise DC/DC converter U14 to generates negative voltage -4.1V for powering analog multiplexers and operational amplifiers. This part is optional, when not used on the board the negative voltage can be supplied from J2:14 pin of J2 connector.

The described schematic is based on assumption, that photocurrents can be measured from the any side of photo-strip. To check this hypothesis, the simulation was made, using Microsim

8.0 PSPICE software. The photocurrent generating junctions in the crossings of strips were modeled as ideal current source in parallel with PN diode. To simplify calculations the sensor model size was chosen 8x8 instead of 64x64. As the real sensor strip has resistance about 50k, to simulate this distributed resistance, between each pare of junctions is connected a 6k resistor. The manufacturer supplied multiplexer and OA PSPICE models were used (almy-sim scheme). To compare signals from the odd and even numbered strips, the illuminated (current generating) area was chosen of square shape 3x3 junctions with the same current value. The simulation results are presented on sim-plot.pdf. Readout time for each strip is equal 25us, so on the time (horizontal) axis we have 8 zones. The square marked curve is for Y, and diamond marked - for X. On the Y plot to illuminated strips correspond to zones 2...4 (from 25us to 100us), on X plot to zones 6...8 (from 125us to 200us). At the beginning of each zone we have large transients, caused by stray capacitance of multiplexers and amplifier settling processes. Apparently the transients for odd and even strips have different shapes. But settled values at the end of each zone are equal with more than 4 decimal digit precision. According to this plots, sampling for AD conversion is made at the end of each zone. For the real sensor duration of zone (including safety margins) is set by the microcontroller software and is chosen about 70us and can be made even smaller without affecting precision.

ALMY-V-IFC (see almy-v-ifc scheme) board contains microcontroller with corresponding auxiliary parts, power supply section and 3 optional interface circuits.

* As the main microcontroller is used Atmel 8-bit AT90S8515 controller chip, having on-chip 8Kbyte Flash program memory, 512 Data EEPROM and 512 SRAM. Flash and EEPROM can be programmed in-site, using serial SPI interface connection through J2:15...J2:20 pins. The EEPROM can be reprogrammed by the microcontroller software, and can be used to store sensor's address (instead of hardware switches or jumpers), correction coefficients (if needed) and any other sensor-dependent information. In future, this chip can be replaced with Atmel Atmega161 with the same pin-out. This new part has capability to be reprogrammed in-site through the same interface, which is used to communicate with the main computer (RS232, RS485 or CANbus, see below). The U5 IC is used to generate RESET signal when supply voltage falls below 4V, preventing possible corruption of EEPROM contents. The clock frequency for the sensor can be optionally generated by on-chip generator, using Y1 quartz, or by external quartz generator Y2. The frequency depends on chosen interface. Typically it is equal 7.3728 MHz for RS interfaces and 16MHz or 8MHz for CANbus.

* Power supply section consists of low-dropout regulator U7, which is adjusted by R6, R17 divider for 4.5V output voltage, voltage dropping circuit D2, R20, to generate about 4.2V voltage for the analog board and optional inductorless DC/DC converter U9 to generate -4.1V for powering the analog board. The chosen voltage values are the optimal to minimize the analog board noise. The main noise sources seem to be analog multiplexers, not sensor and not amplifiers. And the multiplexer noise is rapidly reduced with decreasing of voltage. On the other hand, the minimal voltage rating for the most digital ICs used is 4.5V and maximal difference between analog and digital supply voltages, for good working of microcontroller-ADC interface is 0.3V. The dropout voltage of the U7 chip is very small, so that sensor in whole can be powered by only on 5V...12V external power supply. The voltage of the external supply can be unregulated (well works simple wall transformer), but to minimize the power dissipation inside the sensor, better to use minimal value, but guaranteed not less than 5V on the input

terminals of the sensor (J2:1, J2:5). The current consumption is minimal for the RS485 interface version (less than 40mA when waiting and less than 60mA when transmitting data). So, in case of input voltage 5V, inside the sensor will be dissipated only about 0.2 - 0.3 W.

* As RS232 interface is used Maxim MAX3222 chip, which can work properly at the supply voltages less than 4V.

* As RS485 interface is used Linear Technology LTC1480 IC.

* CANbus interface consists of CAN controller U2 and CAN transceiver U3.

* All connections of the boards are made by two connectors: J1 for stacking connection with the analog board and J2 to connect to the external circuits: power, interface and in-system programmer. J2 is miniature, high density (1.25mm pitch) connector, which has a matching pare with crimp housing, allowing, thus, to connect different terminal wires to different external connectors, depending on the interface type and hardware construction of the sensor in whole.

The software consists of two parts: embedded microcontroller program and PC program. The measurement will be made by the next procedure:

* The main PC switches the laser on and sends broadcasting message to all connected to interface line sensors.

* All sensors simultaneously receiving this message perform the photocurrent measurement for all 128 strips and save result in internal memory.

* The main PC after a necessary for measurement time = number of averaging

* 10ms switches the laser off.

* The main PC afterwards, sequentially address by address reads the data from sensors. If RS485 interface with 115Kbit/sec is used, readout time for one sensor will be about 30ms.

Main advantages of the new design are:
1. Small outline dimensions of the boards: 60x60mm. With the box, assembled sensor will be slightly larger.
2. Much more reliable design: - there are not any contact connections in analog circuits, instead wires are directly bonded to the analog board; - there are not trimming potentiometers used.
3. Instead of very critical regulated power supplies (+8V, -8V, +5V) with separate analog and digital grounds, new sensor needed only one, non-regulated (in range +5...+12V) power supply. It works well even from usual wall transformer.
4. Much less power dissipation: 0.25W (for RS485 interface, Vsuppl = 5V) compared with more than 1.5W of the old one. This parameter is very critical because of laser beam thermal distortions.
5. Only standard components used, not ASIC. So the sensor can be manufactured any time in any quantities.
6. Only 4 layer PCBs, compared with 8 (or 10?) of the old (much cheaper).
7. RS232 standard serial interface for testing and simple applications is available directly on sensor, without external interface board.

8. RS485 standard interface, which will give possibility to connect, using simple cheap adapter (30..50USD), up to 30 sensors to one standard serial port of PC. 10. CANbus interface for more complicated applications.

Future improvements:

The new one with the same size and pinout will replace the AT90S8515 microcontroller: Atmega161, without any changes on the digital board. Using this new controllers we will have new, important, properties.

* Controller will be able to be reprogrammed in-site without SPI in system programming interface, but by using the same main interface with PC, which is used for data acquisition: RS232, RS485 or CANbus. This property maybe especially useful when sensors are used in large setups with hard radiation conditions and limited (if any) possibility for maintenance, to refresh the Flash program memory contents.

* The new controller has hardware multiplication instruction and twice larger program memory. It seems to be possible to have the Gaussian fitting algorithm immediately inside the microcontroller. So instead of 128 2-byte words (total 256 bytes) could be transmitted only 2 4-byte numbers (8 bytes), one for X and one for Y.

The Atmel Corporation claims, that the samples of these new controllers will be available in July 2000.

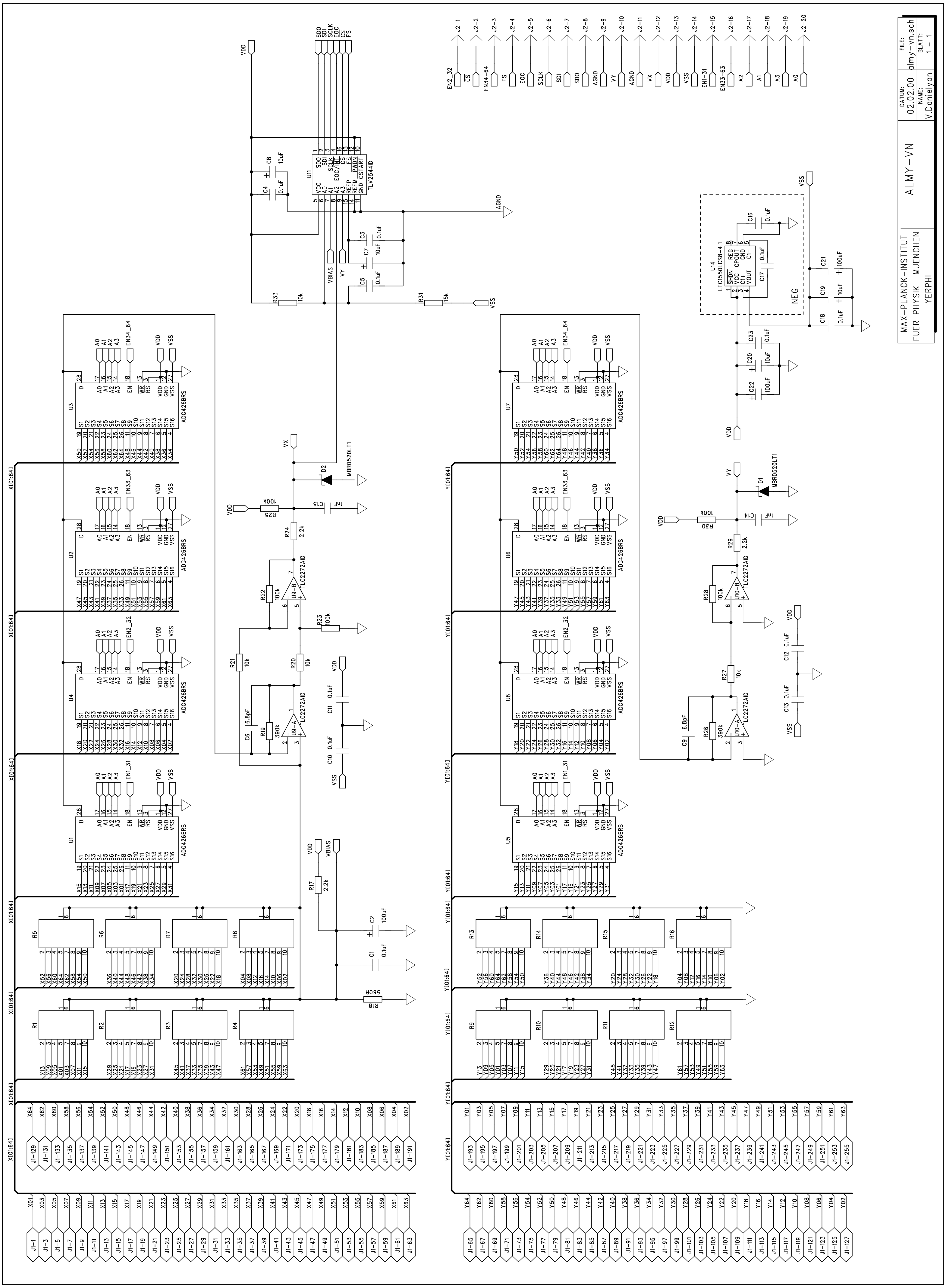
MAX-PLANCK-INSTITUT
FUER PHYSIK MUENCHEN
YERPHI
ALMY-VN
DATUM: 02.02.00
NAME: V.Danielyan
FILE: almy-vn.sch
BLATT: 1 - 1
U11 TLV2544ID
U1 ADG426BRS
U2 ADG426BRS
U3 ADG426BRS
U4 ADG426BRS
U5 ADG426BRS
U6 ADG426BRS
U7 ADG426BRS
U8 ADG426BRS
U9-A TLC2272AID
U9-B TLC2272AID
U10-A TLC2272AID
U10-B TLC2272AID
U14 LTC1550LCS8-4.1
NEG
D1 MBR0520LT1
D2 MBR0520LT1
VDD
VSS
AGND
VX
VY
VBIAS
X[01:64]
Y[01:64]

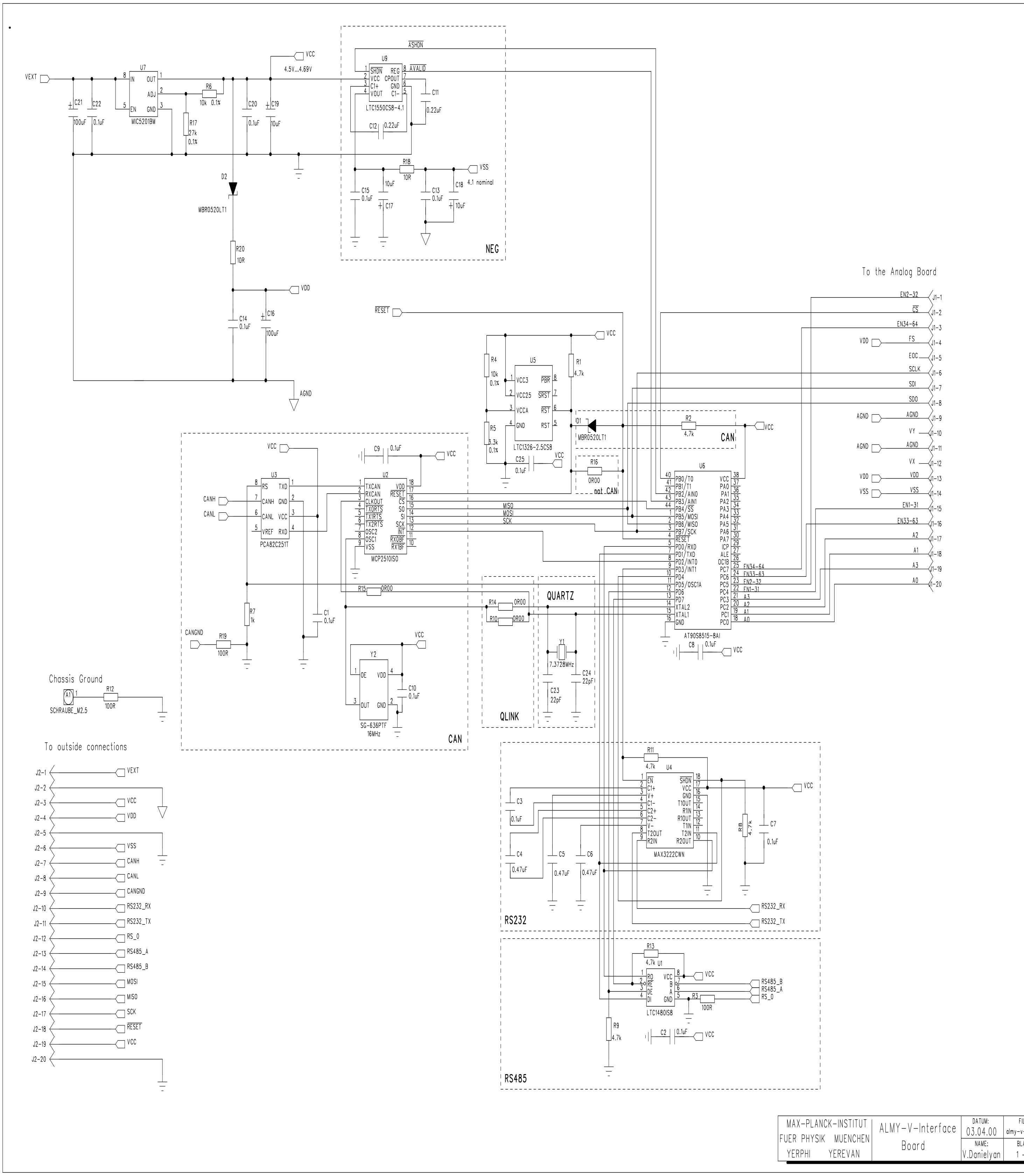
VEXT
U7
MIC5201BM
IN
OUT
ADJ
EN
GND
R6
10k 0.1%
R17
27k
0.1%
C21
100uF
C22
0.1uF
C20
0.1uF
C19
10uF
VCC
4.5V...4.69V
D2
MBR0520LT1
R20
10R
VDD
C14
0.1uF
C16
100uF
AGND
U9
LTC1550CS8-4.1
SHDN
VCC
C1+
VOUT
REG
CPOUT
GND
C1-
AVALID
ASHDN
C11
0.22uF
C12
0.22uF
R18
10R
VSS
4.1 nominal
C15
0.1uF
10uF
C17
C13
0.1uF
C18
10uF
NEG
To the Analog Board
RESET
VCC
R4
10k
0.1%
R5
3.3k
0.1%
U5
LTC1326-2.5CS8
VCC3
VCC25
VCCA
GND
PBR
SRST
RST
R1
4.7k
C25
0.1uF
D1
MBR0520LT1
R2
4.7k
CAN
R16
0R00
not CAN
U6
AT90S8515-8AI
PB0/T0
PB1/T1
PB2/AIN0
PB3/AIN1
PB4/SS
PB5/MOSI
PB6/MISO
PB7/SCK
RESET
PD0/RXD
PD1/TXD
PD2/INT0
PD3/INT1
PD4
PD5/OSC1A
PD6
PD7
XTAL2
XTAL1
GND
VCC
PA0
PA1
PA2
PA3
PA4
PA5
PA6
PA7
ICP
ALE
OC1B
PC7
PC6
PC5
PC4
PC3
PC2
PC1
PC0
EN34-64
EN33-63
EN2-32
EN1-31
A3
A2
A1
A0
C8
0.1uF
EN2-32
CS
EN34-64
FS
EOC
SCLK
SDI
SDO
AGND
VY
VX
VDD
VSS
EN1-31
EN33-63
A2
A1
A3
A0
J1-1
J1-2
J1-3
J1-4
J1-5
J1-6
J1-7
J1-8
J1-9
J1-10
J1-11
J1-12
J1-13
J1-14
J1-15
J1-16
J1-17
J1-18
J1-19
J1-20
VCC
C9
0.1uF
U3
PCA82C251T
RS
CANH
CANL
VREF
TXD
GND
VCC
RXD
CANH
CANL
U2
MCP2510ISO
TXCAN
RXCAN
CLKOUT
TX0RTS
TX1RTS
TX2RTS
OSC2
OSC1
VSS
VDD
RESET
CS
SO
SI
SCK
INT
RX0BF
RX1BF
MISO
MOSI
SCK
R15
0R00
R7
1k
C1
0.1uF
CANGND
R19
100R
Y2
SG-636PTF
16MHz
OE
VDD
OUT
GND
C10
0.1uF
CAN
R14
0R00
R10
0R00
QLINK
QUARTZ
Y1
7.3728MHz
C23
22pF
C24
22pF
Chassis Ground
A1
SCHRAUBE_M2.5
R12
100R
To outside connections
J2-1
J2-2
J2-3
J2-4
J2-5
J2-6
J2-7
J2-8
J2-9
J2-10
J2-11
J2-12
J2-13
J2-14
J2-15
J2-16
J2-17
J2-18
J2-19
J2-20
VEXT
VCC
VDD
VSS
CANH
CANL
CANGND
RS232_RX
RS232_TX
RS_0
RS485_A
RS485_B
MOSI
MISO
SCK
RESET
VCC
R11
4.7k
U4
MAX3222CWN
EN
C1+
V+
C1-
C2+
C2-
V-
T2OUT
R2IN
SHDN
VCC
GND
T1OUT
R1IN
R1OUT
T1IN
T2IN
R2OUT
C3
0.1uF
C4
0.47uF
C5
0.47uF
C6
0.47uF
R8
4.7k
C7
0.1uF
RS232_RX
RS232_TX
RS232
R13
4.7k
U1
LTC1480IS8
RO
RE
DE
DI
VCC
B
A
GND
R3
100R
RS485_B
RS485_A
RS_0
R9
4.7k
C2
0.1uF
RS485
MAX-PLANCK-INSTITUT
FUER PHYSIK MUENCHEN
YERPHI YEREVAN
ALMY-V-Interface
Board
DATUM:
03.04.00
NAME:
V.Danielyan
FIL
almy-v-
BLA
1 -

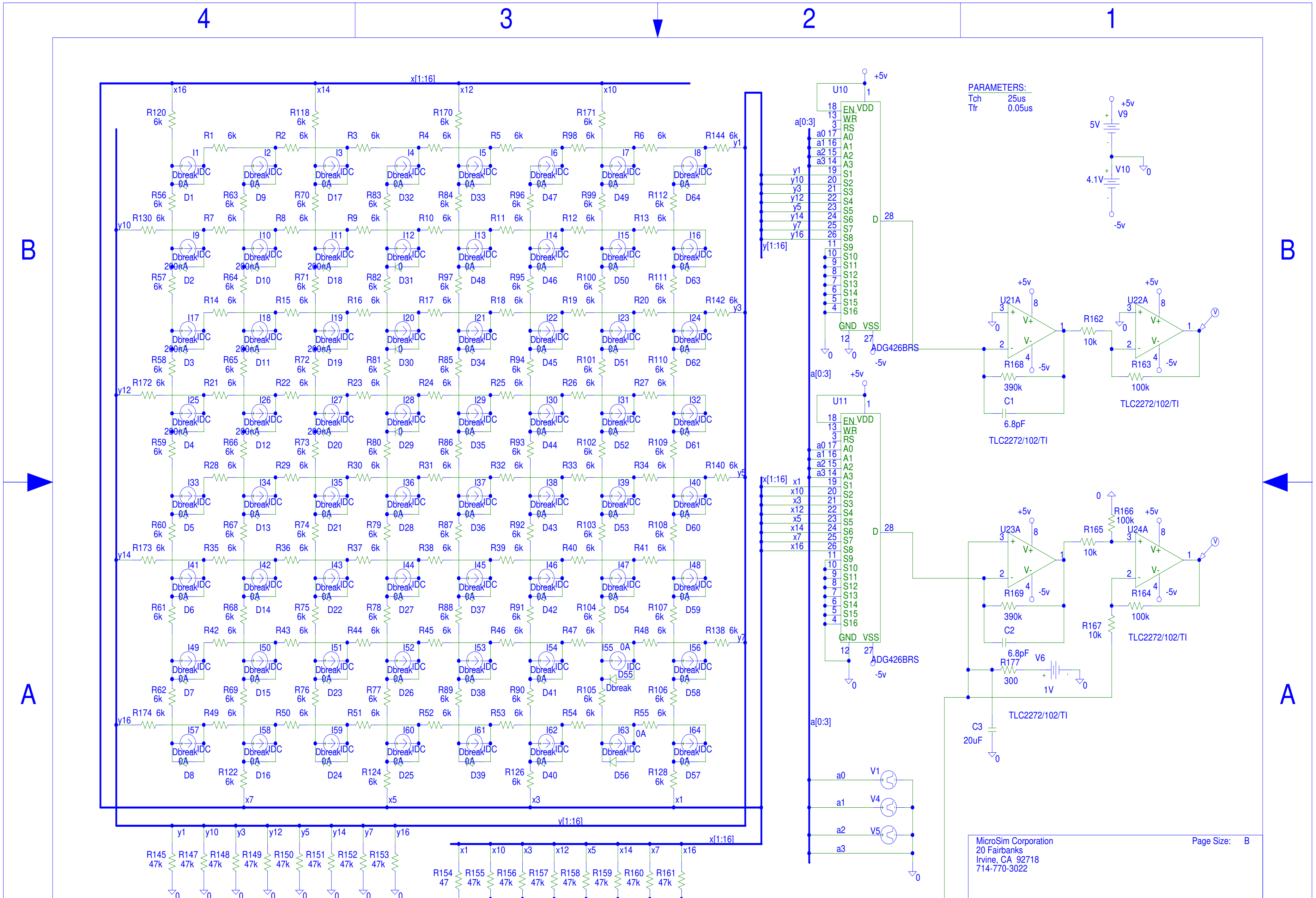
4
3
2
1
B
A
x[1:16]
y[1:16]
a[0:3]
U10
U11
ADG426BRS
EN
WR
RS
A0
A1
A2
A3
S1
S16
D
VDD
GND
VSS
+5v
-5v
PARAMETERS:
Tch 25us
Tfr 0.05us
5V
V9
4.1V
V10
U21A
U22A
U23A
U24A
TLC2272/102/TI
R162 10k
R168 390k
R163 100k
C1 6.8pF
R165 10k
R166 100k
R169 390k
R164 100k
R167 10k
C2 6.8pF
R177 300
V6 1V
C3 20uF
V1
V4
V5
a0
a1
a2
a3
Dbreak
IDC
0A
200nA
6k
47k
MicroSim Corporation
20 Fairbanks
Irvine, CA 92718
714-770-3022
Page Size: B